Am J Physiol Regulatory Integrative Comp Physiol 282: R727–R737, 2002.
First published October 25, 2001; 10.1152/ajpregu.00519.2001.

Molecular cloning and characterization of ryanodine receptor from unfertilized sea urchin eggs

MIEKO SHIWA, TAKASHI MURAYAMA, AND YASUO OGAWA
Department of Pharmacology, Juntendo University School of Medicine, Tokyo 113-8421, Japan

Received 28 August 2001; accepted in final form 25 October 2001

Shiwa, Mieko, Takashi Murayama, and Yasuo Ogawa. Molecular cloning and characterization of ryanodine receptor from unfertilized sea urchin eggs. *Am J Physiol Regulatory Integrative Comp Physiol* 282: R727–R737, 2002. First published October 25, 2001; 10.1152/ajpregu.00519.2001.—Unfertilized eggs of sea urchins (*Hemicentrotus pulcherrimus*) demonstrated cyclic ADP-ribose (cADPR)-induced Ca^{2+} release and caffeine-induced Ca^{2+} release, both of which were considered to be mediated through the ryanodine receptor (RyR). We cloned cDNAs for sea urchin egg RyR (suRyR), which encode a 597-kDa protein of 5,317 amino acids. suRyR shares common structural features with known RyRs: the well-conserved COOH-terminal domain, which forms a functional Ca^{2+} channel, and a large hydrophilic NH_2-terminal domain. suRyR shows amino acid sequence identity (43–45%) similar to the three mammalian RyR isoforms. Phylogenetic analysis indicates that suRyR branched from three isoforms of vertebrates before they diverged, suggesting that suRyR may be the only RyR isoform in the sea urchin. Four in-frame insertions were found in suRyR cDNAs, one of which was novel and unique, in that it had a cluster of serine residues. The transcripts with and without these insertions were found in the egg RNA. These results suggest that suRyR may be expressed as a functional Ca^{2+}-induced Ca^{2+} release channel, which might also be involved in cADPR-induced Ca^{2+} release.

cyclic adenosine 5′-diphosphate-ribose; calcium release channel; endoplasmic reticulum; fertilization

CALCIUM RELEASE from the intracellular stores in sea urchin eggs leads to formation of a fertilization membrane and subsequent developmental processes (52). Recent studies have shown three distinct Ca^{2+} release pathways in these eggs, which are triggered by inositol 1,4,5-trisphosphate (IP_3), nicotinic acid adenine dinucleotide phosphate, and cyclic ADP-ribose (cADPR) (22). The cADPR-induced Ca^{2+} release was potentiated by divalent cations (Ca^{2+} or Sr^{2+}) and caffeine and blocked by ruthenium red, Mg^{2+}, and ryanodine (13, 23), all of which are well-known modulators of Ca^{2+}-induced Ca^{2+} release (CICR) (7) through the ryanodine receptor (RyR), a Ca^{2+} release channel in the endoplasmic reticulum (ER) (10, 31, 44). These findings strongly suggest that the cADPR-induced Ca^{2+} release is mediated by an RyR-like molecule and that the cADPR sensitizes the molecule to Ca^{2+} to activate the channel (22). It was found that cADPR-induced Ca^{2+} release requires calmodulin (CaM) for its activation (24, 48). In addition, photoaffinity labeling of the ^{32}P-labeled cADPR analog identified 100- and 140-kDa proteins as the putative cADPR receptor (51). It is therefore speculated that the RyR-like molecule may form a Ca^{2+} release channel complex with such accessory proteins (22). To understand the molecular mechanisms of cADPR-induced Ca^{2+} release, it is essential to identify these molecules.

RyR has been identified in various animals by molecular cloning for its cDNA. In mammalian cells, there are three genetically distinct isoforms of RyR: RyR1, RyR2, and RyR3 (15, 29, 47). Homologs to mammalian RyRs have also been isolated in nonmammalian vertebrates, e.g., frog (34), chicken (33), and fish (9). RyRs in invertebrates, including *Drosophila melanogaster* (46) and *Caenorhabditis elegans* (40), were recently cloned and sequenced. All the known RyRs showed common characteristics in their primary structure of a hydrophobic transmembrane domain at the COOH terminus and a large NH_2-terminal hydrophilic domain (47). The COOH-terminal domain is predicted to contain at least four transmembrane segments and to form the pore of the Ca^{2+} release channel; the NH_2-terminal domain extends into the cytoplasm to constitute the "feet" structure and may regulate the channel activity (31, 44). cADPR-induced Ca^{2+} release through RyR was also reported in mammalian tissues, although it is controversial in some tissues (11, 32). The cADPR-induced Ca^{2+} release was reported with limited isoforms of RyR2 and RyR3 (22).

Several attempts have been made to identify the RyR-like molecule in sea urchin eggs (25, 28, 35). Using anti-skeletal muscle RyR antibody, McPherson et al. (28) detected an ~380-kDa immunoreactive protein in the cortices of eggs. This indicates that the RyR-like molecule may be localized at the cortical ER, a Ca^{2+} release site, on fertilization. Single-channel recording studies using planar lipid bilayers displayed cADPR-sensitive high-conductance cation channel currents in egg microsomes (25, 35). These currents were activated by Ca^{2+} and blocked by ruthenium red (35) or modified

Address for reprint requests and other correspondence: T. Murayama, Dept. of Pharmacology, Juntendo University School of Medicine, 2-1-1 Hongo, Bunkyo-ku, Tokyo 113-8421, Japan (E-mail: takashim@med.juntendo.ac.jp).

The costs of publication of this article were defrayed in part by the payment of page charges. The article must therefore be hereby marked "*advertisement*" in accordance with 18 U.S.C. Section 1734 solely to indicate this fact.

 0363-6119/02 $5.00 Copyright © 2002 the American Physiological Society

by ryanodine (25), suggesting the existence of RyR-like channels in sea urchin eggs.

In this study, we attempted to identify RyR in sea urchin eggs by cloning and sequencing its cDNA. Homogenates of unfertilized sea urchin eggs demonstrated cADPR-induced Ca^{2+} release and caffeine-induced Ca^{2+} release, both of which were considered to be mediated through RyR. A combination of RT-PCR and cDNA library screening isolated a group of cDNAs for sea urchin RyR (suRyR) from the eggs . The cDNAs encode a 5,317-amino acid protein, which shares common structural features with known RyRs. Our results suggest that sea urchin eggs express RyR as a functional CICR channel, which might also be involved in the cADPR-induced Ca^{2+} release.

MATERIALS AND METHODS

Materials. Sea urchins (*Hemicentrotus pulcherrimus*) were obtained from the Marine Biosystems Research Center, Chiba University (Amatsu-Kominato, Japan). cADPR was enzymatically synthesized from NAD^+ by *Aplysia* ADP-ribosyl cyclase and purified using a Dowex AG1-X2 resin according to the method of Jacobson et al. (17). A contaminating Ca^{2+} was removed through a Dowex 50-X8 resin. The purified cADPR was >98% pure by HPLC.

Ca^{2+} release measurement from sea urchin egg homogenates. Ca^{2+} uptake by and release from Ca^{2+} stores was monitored in egg homogenates by fluorometrically determining free Ca^{2+} concentration ($[Ca^{2+}]$) in the medium (23). Unfertilized eggs from *H. pulcherrimus* were homogenized in 4 vol of a medium containing 250 mM potassium gluconate, 250 mM *N*-methylglucamine, 20 mM HEPES, and 1 mM $MgCl_2$, pH 7.2, according to the method of Clapper and Lee (4). The homogenate (150 μl) was added to a fluorometer cuvette containing 1.5 ml of the above medium supplemented with 5 mM phosphocreatine, 2 U/ml of creatine kinase, and 3 μM fluo 3. Exogenous CaM was not necessary for Ca^{2+} release by cADPR with this system, suggesting that a sufficient amount of CaM may be contained in this homogenate. The cuvette was set in a Hitachi F-4500 fluorescence spectrofluorometer and incubated at 30°C. Fluo 3 fluorescence was measured with excitation and emission wavelengths of 488 and 525 nm, respectively. Because $[Ca^{2+}]$ in the cuvette reached ≥10 μM in the presence of the homogenate, no extra Ca^{2+} was added. Ca^{2+} uptake was started by addition of 1 mM Mg-ATP and reached the steady state in 5–10 min. At this point, cADPR or caffeine was added and the time-dependent changes in fluo 3 fluorescence were monitored.

Isolation of total and poly(A)$^+$ RNA. Total RNA was extracted from the unfertilized eggs of several *H. pulcherrimus* by the guanidine isothiocyanate-cesium chloride method (3), and poly(A)$^+$ RNA was isolated through an oligo(dT)-cellulose column (Amersham Pharmacia Biotech). For Northern blot analysis, poly(A)$^+$ RNA was similarly prepared from bullfrog skeletal muscle.

Cloning of suRyR cDNA. A combination of RT-PCR and cDNA library screening was carried out to isolate the cDNA encoding suRyR. The first-strand cDNA was generated from poly(A)$^+$ RNA by a Superscript II cDNA kit (GIBCO BRL) with oligo(dT) and random primers according to the manufacturer's instructions. The PCR step was performed with the degenerate primers that were designed on the basis of the published cDNA sequences of various vertebrate and invertebrate RyRs. Seven PCR products corresponding to the suRyR cDNA sequence were obtained: R1 (402–1587), R2 (1451–1841), R3 (2983–3719), R4 (8637–9420), R5 (9247–9536), R6 (13510–14942), and R7 (14985–15804).

Oligo(dT) and randomly primed cDNA libraries were prepared from poly(A)$^+$ RNA and constructed in λZAP II vector (Stratagene). These cDNA libraries were screened with the above PCR fragments, and a positive insert was subcloned into a pBluescript SK(−) vector. Two cDNA clones, P5 [13910–3′-untranslated region (UTR)] and P7 (14176–3′-UTR), were obtained from the oligo(dT) cDNA library; 13 cDNA clones, P1 (2223–4168), P2 (8807–11679), P3 (−669–746), P4 (9114–14291), P6 (989–2532), P14 (−651–459), P17 (8142–11321), P19 (−533–2923), P20 (892–3202), P21 (2496–5243), P24 (−17–1573), P26 (−629–1172), and P27 (7258–9987), were obtained from the randomly primed cDNA library. Six additional clones, P28 (5776–7717), P29 (6566–9143), P30 (5124–6747), P31 (3741–5732), P32 (7181–9086), and P33 (6515–7748), were obtained by screening the randomly primed library with the 0.5-kbp *Eco*RV fragment (4728–5243) derived from P21 and the 0.8-kbp *Sac*I fragment (7258–8063) from P27. These clones overlapped each other and covered the entire coding region and part of the 5′- and 3′-untranslated regions of suRyR cDNA (see Fig. 2).

Northern blot analysis. Poly(A)$^+$ RNAs from *H. pulcherrimus* eggs and bullfrog skeletal muscle (25 μg each) were electrophoresed on 0.5% agarose-formaldehyde gels and transferred onto Hybond-N$^+$ nylon membranes (Amersham Pharmacia Biotech). cDNA inserts of 3′ regions, P7 and pβFRR01 (34), were used as probes for suRyR and bullfrog β-RyR, respectively. The transferred membranes were hybridized for 16 h at 42°C with the ^{32}P-labeled probe, and the positive bands were detected by autoradiography.

RT-PCR assay for detection of insertion/deletion variants. The first-strand cDNA was generated from 3 μg of total RNA with oligo(dT) primer (GIBCO BRL) and used as a template for the PCR. Within the range of the linear relationship between the initial template and the amplified product, a small amount of the template (1 nl) was used. PCR was carried out with a specific primer pair for each insertion/deletion site using standard protocol of 30 cycles at an annealing temperature of 65°C. The PCR products were electrophoresed on a 2% agarose gel and stained with ethidium bromide. The intensity of the bands was determined with a MasterScan densitometer.

Analysis of cDNA and protein sequences. Nucleotide sequences from individual clones were assembled into a full-length contig with the AssemblyLIGN (version 1.0), and the cDNA and protein sequences were analyzed with MacVector (version 7.0) software (IBI, Kodak). Nucleotide residues are numbered, with the adenine residue in the first initiation codon being expressed as 1. All the possible insertions were included in the full-length cDNA and protein sequences. The hydropathy profile was calculated by the method of Kyte and Doolittle (21) using a window of 19 amino acids. Alignment of RyR sequences was performed by the ClustalW with initial pairwise alignment using the BLOSUM 30 weight table (open and extended gap penalties of 10 and 0.1, respectively). A phylogenetic tree was inferred on the basis of the neighbor-joining method (39), and the probabilities that two lineages are joined at their node to form a single cluster have been estimated by the bootstrap method as a standard procedure with 1,000 resamplings (8). The aligned sequences from 11 RyRs, except for the 3 divergent regions (D1–D3) of less similarity, were used for the phylogenetic analysis, where a type 1 IP_3 receptor was adopted as the out group.

RESULTS

cADPR-induced Ca^{2+} release and caffeine-induced Ca^{2+} release from egg homogenates of H. pulcherrimus. We initially examined whether the sea urchin eggs we used for cDNA cloning actually show cADPR-induced Ca^{2+} release. Figure 1 depicts changes in the fluo 3 fluorescence intensity in the medium containing homogenates prepared from *H. pulcherrimus* eggs. The fluo 3 fluorescence, which reflects [Ca^{2+}], rapidly declined on addition of 1 mM Mg-ATP and reached the steady state within 5 min, indicating that a significant amount of Ca^{2+} was actively loaded into Ca^{2+} stores in the homogenates. At this point, 0.2 μM cADPR produced a transient Ca^{2+} release (Fig. 1*A, left*). An increase in cADPR concentration up to 1 μM increased the amount of released Ca^{2+} with the accelerated rate of rise (Fig. 1*A, left, inset*). The second application of cADPR in the sequence, however, failed to release Ca^{2+}, showing "desensitization," which was one of the reported characteristics of cADPR-induced Ca^{2+} release (5). This is not due to depletion of Ca^{2+} in the stores, because 0.2 μM cADPR on the initial addition was not the maximal dose. Results were similar with addition of exogenous CaM; a sufficient amount of CaM may be contained in this homogenate system. These results suggest that cADPR definitely releases Ca^{2+}

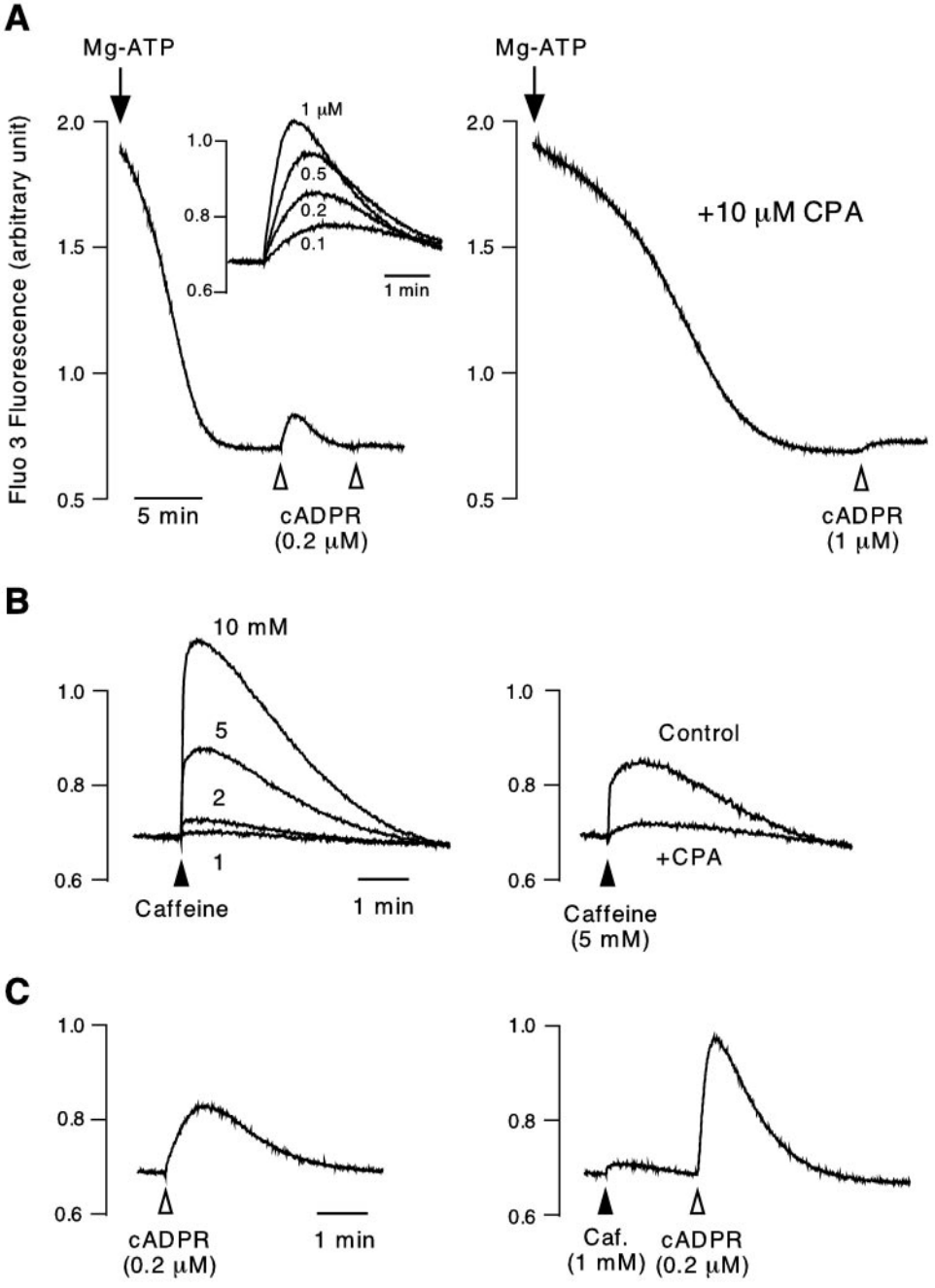

Fig. 1. Cyclic ADP-ribose (cADPR)-induced Ca^{2+} release and caffeine (Caf)-induced Ca^{2+} release from sea urchin egg homogenates. Free Ca^{2+} concentration was monitored with 3 μM fluo 3, and fluorescence intensity is expressed in arbitrary units. *A*: cADPR-induced Ca^{2+} release. Egg homogenates of *H. pulcherrimus* were actively loaded with Ca^{2+} by addition of 1 mM Mg-ATP (arrows). *Left*: application of 0.2 μM (final concentration) cADPR (open arrowheads) induced a transient Ca^{2+} release. The second application of cADPR in the sequence failed to release any Ca^{2+}, showing "desensitization." *Inset*: dose-dependent Ca^{2+} release with 0.2–1 μM cADPR. The Ca^{2+}-releasing effect was maximum at 1 μM, because ≥1 μM cADPR showed similar responses. *Right*: Ca^{2+} uptake was observed even in the presence of 10 μM cyclopiazonic acid (CPA) at a much reduced rate. Ca^{2+} release by 1 μM cADPR, in contrast, was completely lost. *B*: caffeine-induced Ca^{2+} release. Egg homogenates were similarly loaded with Ca^{2+} and stimulated by various concentrations of caffeine (closed arrowheads). Caffeine at ≥2 mM demonstrated a transient Ca^{2+} release in a dose-dependent manner (*left*). Treatment with 10 μM CPA greatly inhibited Ca^{2+} release (*right*). *C*: effect of caffeine on cADPR-induced Ca^{2+} release. Application of the threshold concentration of caffeine (1 mM, closed arrowheads) markedly potentiated the Ca^{2+} release by subsequent addition of 0.2 μM cADPR (*right*) compared with the control experiment (*left*).

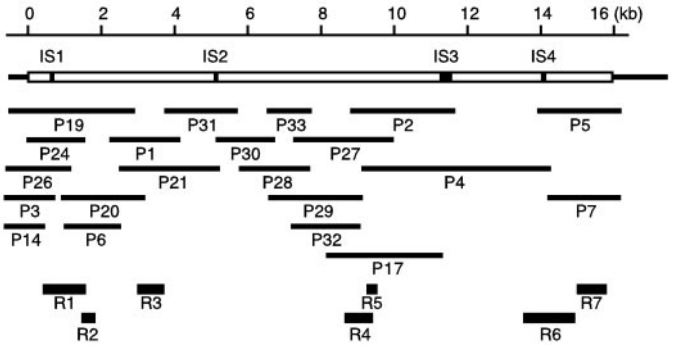

Fig. 2. Map of sea urchin ryanodine receptor (suRyR) cDNA clones. *Top row*: full-length suRyR cDNA with the open reading frame (ORF) as an open box. Four possible insertion/deletion sites (IS1–IS4) are shown in black. Thin lines (P1-P33) represent isolated suRyR cDNA clones, in which P5 and P7 were obtained from oligo(dT)-primed cDNA library and the others were from the randomly primed library. Bold lines (R1–7) indicate the cDNA fragments that were obtained by RT-PCR and used as probes in screening the cDNA libraries.

from *H. pulcherrimus* sea urchin eggs. In the presence of 10 μM cyclopiazonic acid (CPA), an inhibitor of ER Ca^{2+}-ATPase, Ca^{2+} uptake proceeded, but at a much reduced rate (Fig. 1*A, right*). Because this uptake was inhibited by 5 mM sodium azide, an inhibitor of mitochondrial Ca^{2+} uptake, it can be concluded that the Ca^{2+} loading was mainly performed by mitochondria. Under this condition, 1 μM cADPR, which showed the maximum Ca^{2+} release, failed to release Ca^{2+}. Similar results were obtained in the presence of 1 μM thapsigargin (data not shown). Addition of 5 mM sodium azide alone also retarded Ca^{2+} loading, but the cADPR-induced Ca^{2+} release was definitely observed (data not shown). Therefore, Ca^{2+} loading was primarily carried out by ER and mitochondria, but the cADPR-sensitive Ca^{2+} store is the ER.

Caffeine is a well-known Ca^{2+}-releasing agent that potentiates CICR by activating RyR (31). Caffeine at ≥2 mM induced a transient Ca^{2+} release from the egg homogenates in a dose-dependent manner (Fig. 1*B, left*). Ca^{2+} release was inhibited by treatment with 10 μM CPA, indicating that the source of Ca^{2+} released by caffeine is the ER. These results suggest that the egg homogenates may have a CICR mechanism, which in turn implies the presence of RyR.

In this egg homogenate system, ER is the source of Ca^{2+} for cADPR-induced Ca^{2+} release and caffeine-induced Ca^{2+} release (Fig. 1, *A* and *B*). In addition, application of the threshold concentration of caffeine (1 mM) greatly potentiated the Ca^{2+} release triggered by subsequent addition of cADPR (Fig. 1*C, right*) compared with the control experiment without caffeine (Fig. 1*C, left*). Thus the cADPR-induced Ca^{2+} release in *H. pulcherrimus* eggs shares common properties with caffeine-induced Ca^{2+} release, suggesting that the cADPR-induced Ca^{2+} release may be mediated through RyR (22).

Cloning of suRyR cDNA. Cloning of cDNA for suRyR was carried out in two steps. Initially, seven short DNA fragments (PCR1–7) were obtained by RT-PCR with the degenerated primers designed according to the reported RyR sequences. Using these fragments as a probe for cDNA library screening, we then isolated a total of 21 overlapping clones (see MATERIALS AND METHODS). A set of cDNA clones contained a continuous 15,954-bp open reading frame (ORF) sequence, in addition to 669-bp 5′-noncoding and ~1.9-kbp 3′-noncoding regions (Fig. 2). A nucleotide sequence, CGACCATGG, that closely resembles the consensus initial sequence CA(G/A)CCATGG (19) was found around the initiation codon. A termination codon TAA existed 15 bp upstream from the first methionine codon. A typical polyadenylation signal, AATAAA (36), was located 36 bp upstream of the polyadenylation site.

During sequencing of these clones, a number of nucleotide differences became apparent between overlapping clones. A total of 94 nucleotide substitution sites were found in the ORF; only 8 disclosed amino acid substitution, and the others were silent. The sites with amino acid substitution are listed in Table 1. Because of their majority (>90%), these silent substitutions would be caused by polymorphism of the sequence, which might be partly ascribed to some heterogeneous RNA samples prepared from eggs of different sea urchins. Analysis of overlapping clones also revealed the nucleotide stretches of tens or more nucleotides that are missing in some clones. Such stretches were detected at four sites (IS1–IS4) in the ORF (Table 2). The numbers of nucleotides are multiples of three in all the stretches, indicating that they will not cause any frame

Table 1. *Nucleotide substitution sites that cause amino acid substitution in suRyR cDNA*

Nucleotide Position	Nucleotide Substitution	Amino Acid Substitution
316	AGC→GGC	S^{106}→G
865	CCC→GCC	P^{289}→A
2150	GTT→GGT	V^{717}→G
2237	CTC→CCC	L^{746}→P
2518	CAC→GAC	H^{840}→D
2899	CTG→ATG	L^{967}→M
3775	ATG→TTG	M^{1259}→L
10705	ACT→GCT	T^{3569}→A

Substituted nucleotides are indicated by an underline. The number of A in the initial methionine codon represents 1. Amino acids are written in one-letter code with their position in the amino acid sequence. suRyR, sea urchin ryanodine receptor.

Table 2. *Insertion/deletion sites in suRyR cDNA*

			cDNA Clones	
Name	Nucleotide	Amino Acid	With IS	Without IS
IS1	626–658 (33)	A^{209}–L^{219} (11)	P3, P24, P26	P19
IS2	5105–5164 (60)	I^{1702}–Q^{1721} (20)	P21, P30	P31
IS3	11248–11574 (327)	V^{3750}–T^{3858} (109)	P2, P17	P4
IS4	14065–14121 (57)	N^{4689}–M^{4707} (19)	P5	P4

Amino acids are written in one-letter code with their position in the amino acid sequence. Numbers in parentheses represent length of nucleotides or amino acids in insertion/deletion site.

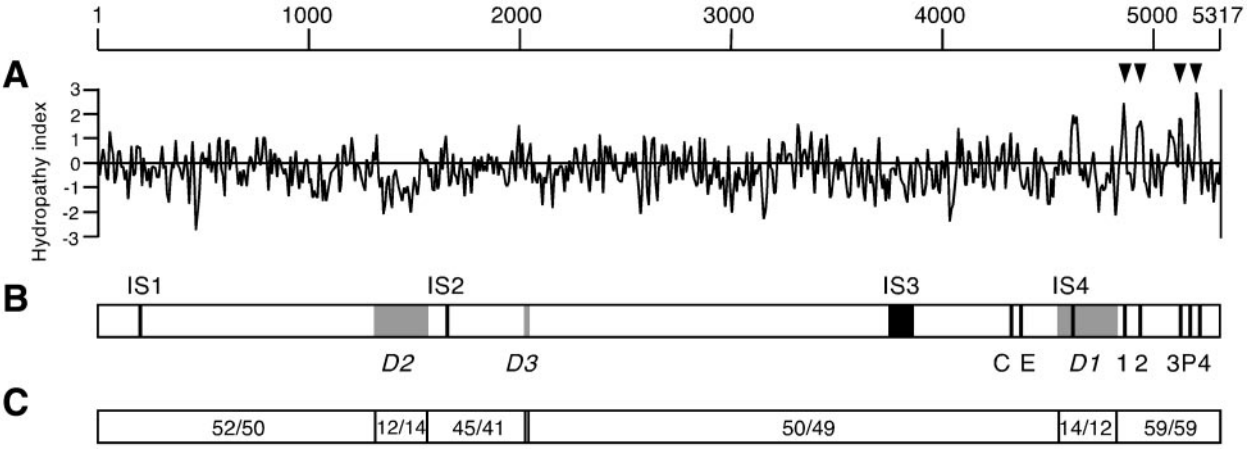

Fig. 3. Analysis of suRyR structure. *A*: hydropathy profile of sea urchin egg RyR. The profile was made by the algorithm of Kyte and Doolittle (21) with a window of 19 amino acids. Four highly hydrophobic segments are indicated by arrowheads. *B*: domain structure of suRyR. Three divergent regions (D1–D3) (43) are indicated by the gray box. The four hydrophobic segments (arrowheads in *A*), which correspond to putative transmembrane segments (M1–M4) (47), are represented by numbered vertical bars, together with a pore-forming segment (P) (55). The conserved glutamate residue involved in the Ca^{2+} sensor (2) is represented as C and 2 EF-hand motifs (53) (bold vertical bar) as E. Four potential insertion sites (IS1–IS4) are also shown. *C*: amino acid sequence of suRyR is aligned with sequences of rabbit RyR2 (29) and *D. melanogaster* RyR (46) for comparison. Calculated percent identities in amino acid sequences segmented arbitrarily by D1, D2, and D3 are shown as suRyR vs. RyR2/suRyR vs. *D. melanogaster* RyR.

shift. These stretches may be potential insertion/deletion sequences.

Analysis of suRyR sequence and comparison with known RyRs. The suRyR cDNA encodes a sequence of 5,317 amino acids with molecular weight of 597,181 when four potential insertions are present. Deletion of all the insertions will generate a 5,158-amino acid protein (mol wt = 580,566). The structural features of suRyR are demonstrated in Fig. 3. The hydropathy profile revealed that there are four highly hydrophobic segments (4845–4866, 4930–4953, 5118–5137, and 5194–5220) in one-tenth of the COOH terminus (Fig. 3*A*) and that the remaining large part is hydrophilic. This characteristic is shared by all RyRs reported.

The predicted domain structure of suRyR, which is also common among all RyRs reported, is shown in Fig. 3*B*. Alignment of suRyR with other RyRs showed two regions (1312–1559 and 4549–4835) with markedly low identity (<20%), corresponding to known divergent regions, D2 and D1, respectively (43). The D3 region of suRyR (2023–2032) was shorter than its counterpart (40–50 amino acid residues) of the vertebrate RyRs (43).

The identities in the entire amino acid sequence among vertebrate and invertebrate RyRs are listed in Table 3. The scores of identity for suRyR were similar (43–45%) to any one of the three rabbit RyR isoforms (RyR1–3). Identities of suRyR with RyRs from *D. melanogaster* and *C. elegans* were 43 and 39%, respectively. These scores were markedly lower than those among genetically distinct RyR isoforms of vertebrates (65–67%) or between corresponding isoforms of mammals and frogs (≥80%) (34). The identities of the restricted regions of suRyR with the corresponding counterparts of rabbit RyR2 and *D. melanogaster* RyR are shown in Fig. 3*C*. The highest identity was observed in the COOH-terminal region (59%). Two regions, the NH_2 terminus and the stretch between D3 and D1, follow in identity (49–52%), which is slightly higher than overall identity (43–45%). In contrast, only 12–14% identity was observed at D1 and D2. It is unlikely that suRyR is much more similar to RyR2 or RyR3 than to RyR1 or invertebrate RyRs.

It has been shown that most of the functionally important domains of RyR reside in its COOH-terminal region (1). The COOH-terminal region of suRyR was therefore compared with those of rabbit RyR1–3 (Fig. 4). Four highly hydrophobic segments shown by hydropathy plots (Fig. 3*A*) corresponded to the four putative transmembrane and channel-forming domains (M1–M4) proposed by Takeshima et al. (47) and showed a high similarity to those of other RyRs, especially in M3 and M4. A sequence motif, GXRXGGGXGD, which has been shown to constitute a part of pore-forming segments of the Ca^{2+} release

Table 3. *Percent identities of the amino acid sequences among RyRs*

	rRyR2	rRyR3	suRyR	dmRyR	ceRyR
rRyR1	65	65	43	43	39
rRyR2		67	45	44	40
rRyR3			43	43	38
suRyR				43	39
dmRyR					44

Percent identities between RyRs were calculated from pairwise alignment of the entire amino acid sequences. A continuous stretch of gaps that had been inserted to achieve maximum homology was counted as one substitution regardless of its length. rRyR1–3, rabbit RyR1–3; dmRyR, *D. melanogaster* RyR; ceRyR, *C. elegans* RyR. The scores of identity for suRyR were of similar values (43–45%) with rRyR1–3.

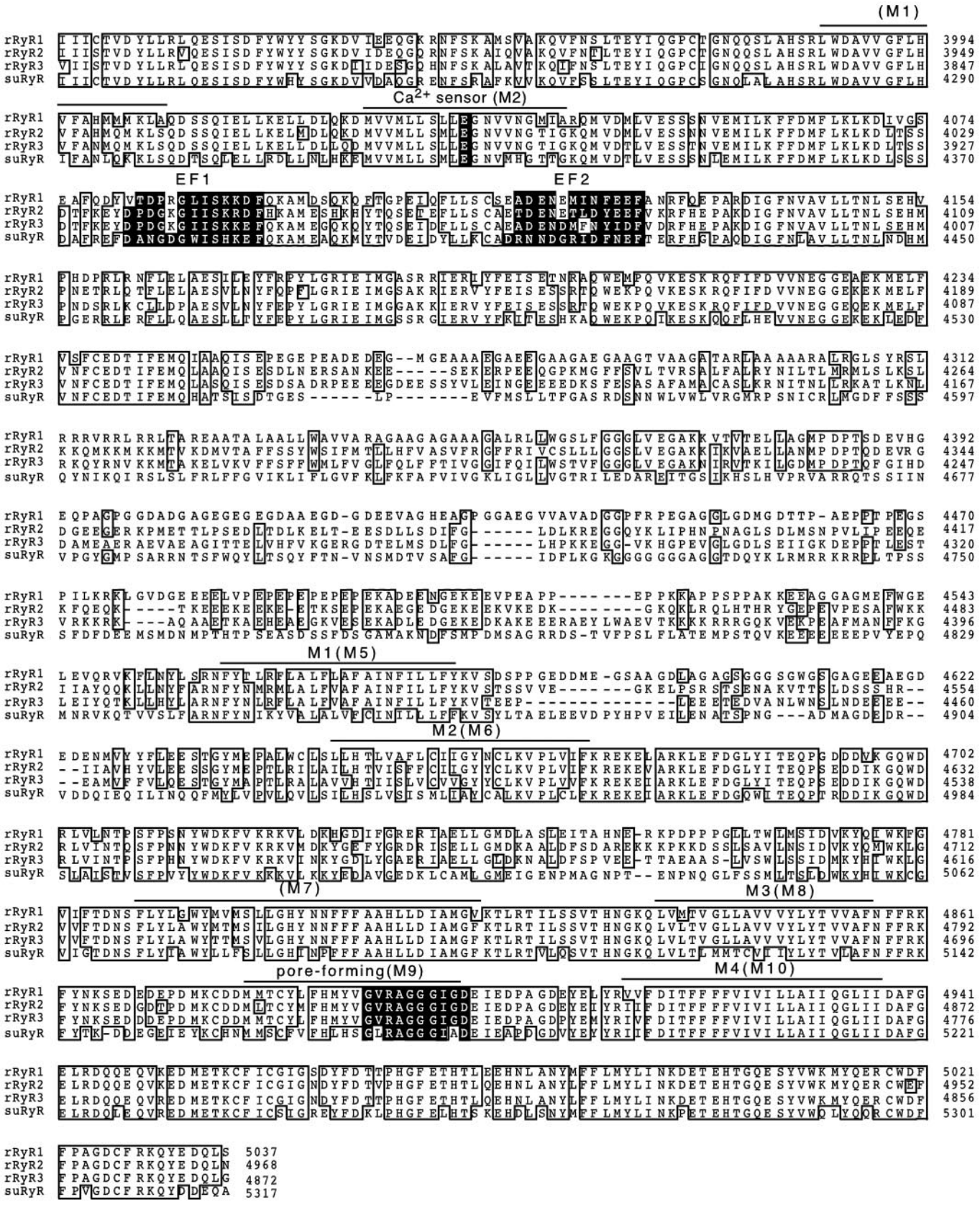
(M1)
Ca2+ sensor (M2)
EF1
EF2
M1(M5)
M2(M6)
(M7)
M3(M8)
pore-forming(M9)
M4(M10)
rRyR1
rRyR2
rRyR3
suRyR

channels (55), was well conserved (5170–5179), except a glycine residue at the ninth position (G^{5178}) was substituted by alanine. In addition, residues corresponding to I^{4897}, R^{4913}, and D^{4917} of rabbit RyR1, which were recently shown to play an important role in activity and conductance of the Ca^{2+} release channel (12), were conserved in suRyR. A glutamate that is proposed to be involved in the Ca^{2+} sensitivity in rabbit RyR3 (E^{3885}) (2) and RyR1 (E^{4032}) (6) was also detected in suRyR (E^{4328}). In addition, motif search with the PROSITE library found two EF-hand motifs placed in tandem in the COOH-terminal region (4377–4389 and 4412–4424), which was originally reported in lobster RyR (53).

A consensus sequence for the putative adenine ring binding domain, Y[GAST][VG][KTQSN], which was reported with chaperonin protein GroES (26), was found in two sites (1096–1099 and 4233–4236). The two sites were well conserved in all known RyRs (31). A consensus sequence for the P-loop ATP/GTP-binding motif, [GA]XXXXGK[ST] (41), was found in the NH_2-terminal region (1150–1157). An RGD motif corresponding to R^{3499}GD of rabbit RyR1, which was proposed to be involved in excitation-contraction coupling in skeletal muscle (31), was not conserved (P^{3684}DG), although an RGD was found in another site (1732–1734). A potential apo-CaM and Ca^{2+}-CaM binding site was recently identified in mammalian RyR1 (3614–3643 of rabbit RyR1) (38, 54). The corresponding site was well conserved in suRyR (3911–3940). In addition, there were five putative sites (267–279, 1090–1103, 3222–3235, 4617–4631, and 4995–5007) for consensus motifs for Ca^{2+}-dependent CaM binding (1-8-14 and 1-5-10 motifs) (37), but no IQ motif was found as a consensus for Ca^{2+}-independent CaM binding (37). Leucine/isoleucine zipper motifs in RyR, the occurrence of which has been demonstrated (31), were recently proposed to be a protein kinase and phosphatase binding domain via kinase/phosphatase targeting proteins (27). Two of the motifs (554–593 and 3218–3254) were well conserved in suRyR, whereas one (1764–1803) was less homologous.

A notable feature of the suRyR sequence was found in the IS3 insertion (3750–3858), located near one-fourth of the distance from the COOH terminus. This insertion was considerably large and characterized by a cluster of serine residues (Fig. 5). Of 109 residues, 40 serine residues (37%) were found, and most of them were located in the middle of the sequence. Several consensus motifs for protein phosphorylation sites (18) were observed around the serine cluster. The corresponding insertion sequence was not reported in any other RyRs. Furthermore, BLAST search failed to find homologous sequences in the protein database. Thus the IS3 insertion is an entirely unique sequence in suRyR.

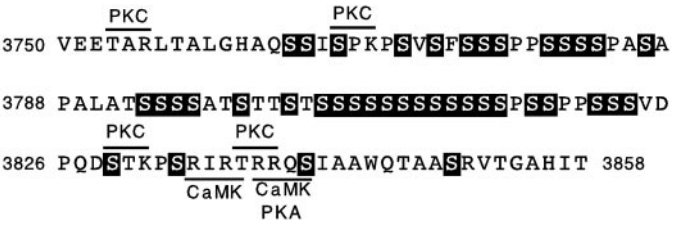

Fig. 5. Characteristic amino acid sequence of IS3 insertion in suRyR. Serine residues are expressed as inversed. Putative phosphorylation sites for Ca^{2+}/calmodulin (CaM)-dependent protein kinase II (CaMK), cAMP-dependent protein kinase (PKA), and protein kinase C (PKC) are indicated. Serine residues are clustered in the middle of the sequence, and putative phosphorylation sites are located around the cluster for the serine residues.

Phylogenetic analysis of the RyR family. To learn the evolutionary relationship between suRyR and the other RyRs, we carried out phylogenetic analysis of the RyR family (Fig. 6). A phylogenetic tree was obtained as the result of an alignment of amino acid sequences of 11 RyR species and the type 1 IP_3 receptor as the out group (see MATERIALS AND METHODS). The tree is presented in the form of a dendrogram and exhibits evolutionary divergence from a putative ancestral RyR and subsequent ancestors (nodes), with branch length indicating the degree of sequence divergence from the predicted ancestor. It first branched into two nodes, one of which included *D. melanogaster* and *C. elegans,* which belong to protostomes, and the other for deuterostomes, including the vertebrates and sea urchins. suRyR subsequently branched from the ancestors of vertebrate RyRs. Branching of *D. melanogaster* and *C. elegans* also seems to have occurred at about the same time. Then the three vertebrate isoforms (RyR1, RyR2, and RyR3) appear to have diverged. These results agree well with the evolution of animals as predicted by classical systematics. The fact that the three vertebrate isoforms diverged after branching of suRyR also suggests the presence of a single isoform of RyR in the sea urchin (i.e., suRyR only), as is the case with other invertebrates (40, 46).

Analysis of suRyR transcripts in unfertilized eggs. Northern blot analysis for the suRyR transcripts in unfertilized sea urchin eggs is shown in Fig. 7*A*. Only a large transcript signal was detected, which shows lower mobility than for β-RyR from frog skeletal muscle (16.0 kbp; Fig. 7*B*). The size of the transcript was estimated to be >18 kbp, which agrees well with that predicted by the full-length cDNA (18.5 kbp).

Fig. 4. Alignment of the COOH-terminal region of suRyR protein sequence with those of vertebrate RyRs. A sequence of suRyR is aligned with sequences of RyR1 (47), RyR2 (29), and RyR3 (15) of rabbit (rRyR1–3). Putative transmembrane segments (M1–M4) proposed by Takeshima et al. (47) are shown by thin lines; M1, M2, and M5–M10 in parentheses represent those suggested by Zorzato et al. (56). A glutamate residue in (M2), which is proposed to serve as the Ca^{2+} sensor (2), is indicated as inversed. Two EF-hand motifs aligned in tandem (EF1 and EF2) (53) are also shown; residues corresponding to consensus EF-hand motif (20) are inversed. Conserved residues for the putative pore-forming segments GXRXGGGXGD (55) around (M9) are indicated as inversed.

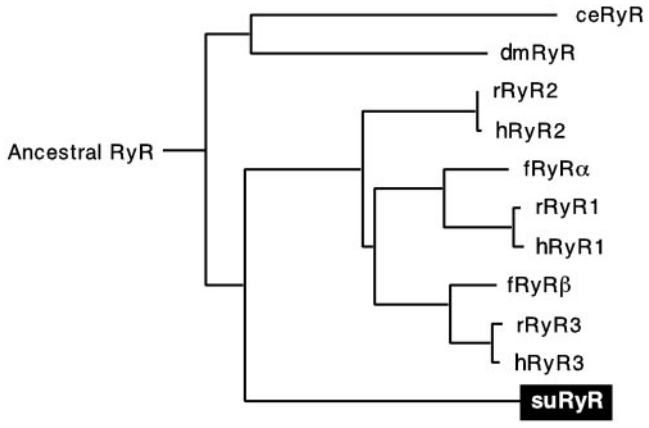

Fig. 6. Phylogenetic tree of the RyR family. A phylogenetic tree was obtained from the optimal alignment of 11 RyR sequences, with a type 1 inositol 1,4,5-trisphosphate receptor adopted as the out group. The 3 divergent regions were omitted from the alignment. Length of horizontal lines is proportional to the number of amino acid substitutions. hRyR1–3, human RyR1–3; rRyR1–3, rabbit RyR1–3, fRyRα, frog α-RyR; fRyRβ, frog β-RyR; dmRyR, *D. melanogaster* RyR; ceRyR, *C. elegans* RyR. suRyR branched from vertebrate RyRs after their branching from *D. melanogaster* and *C. elegans* RyRs.

To determine the expression pattern of potential insertion/deletion variants of suRyR in sea urchin egg, we used specific primer pairs for each insertion site to amplify the variant transcripts by RT-PCR. Figure 8*A* shows the result for IS3. cDNA clones P2 and P4 were used as a control for insertion and deletion variants, respectively (Table 2). The egg total RNA gave rise to two bands with mobilities that corresponded to those of P2 and P4, respectively, indicating that these transcripts exist in sea urchin eggs. The intensity of the band for the insertion variant was estimated to be 11% of total (insertion + deletion) intensity. The population of the insertion variant should be ≤6% of the total after correction for the mass of products (562 vs. 235 bp). Similar analysis was done for the other three sites (Fig. 8*B*). About two-thirds were insertion variants in IS1,

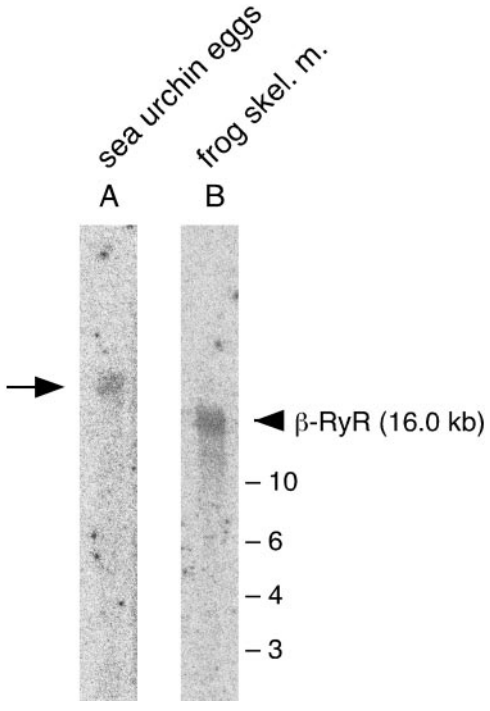

Fig. 7. Northern blot analysis of suRyR RNA from unfertilized sea urchin eggs. Poly(A)$^+$ RNA (25 μg each) from sea urchin eggs (*A*) and bullfrog skeletal muscle (*B*) was separated on 0.5% formaldehyde-agarose gels, transferred to nylon membranes, and hybridized with ^{32}P-labeled DNA probe for suRyR and β-RyR, respectively. Position and size (in kbp) of markers are indicated at *right*. Hybridized band (arrow) from sea urchin eggs showed a significantly smaller mobility than 16-kbp β-RyR mRNA (arrowhead) from bullfrog skeletal muscle, being consistent with the large size (18.5 kbp) of the full-length cDNA.

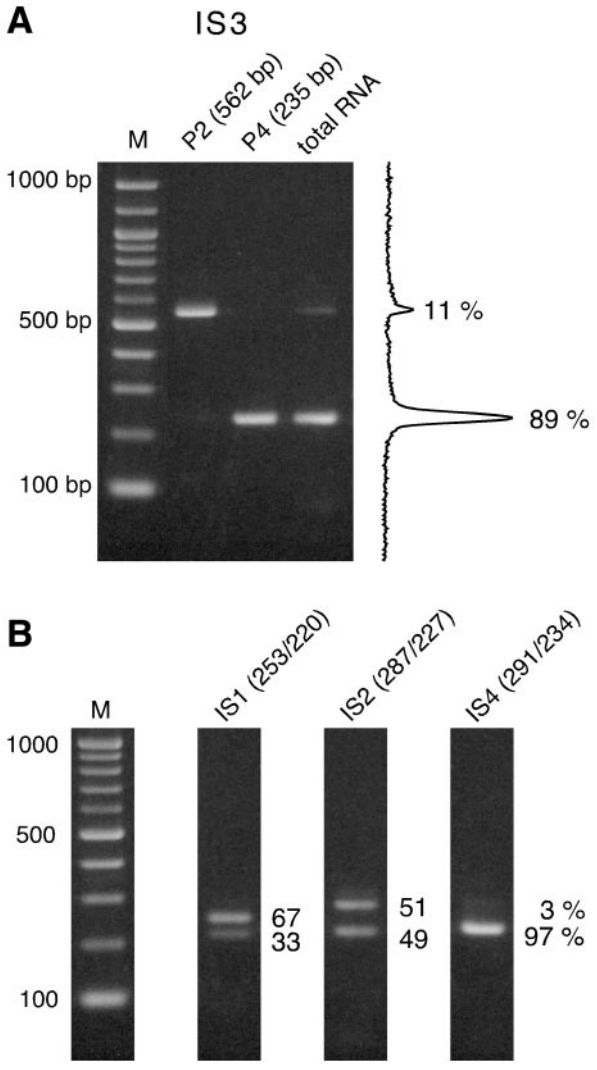

Fig. 8. Estimate of the fraction of insertion/deletion variants of suRyR by RT-PCR. Unfertilized sea urchin egg total RNA was reverse transcribed using oligo(dT) primer and subjected to PCR using a specific pair of primers for each insertion/deletion site. *A*: result for IS3. PCR was also done with clones P2 and P4 as a template for size control with and without insertion, respectively (Table 2). Numbers in parentheses represent estimated size of PCR product. Densitometric profile is shown on *right*. The ratio of intensity of each band to the total is indicated. Population of insertion variant should be ≤6% of the total suRyR transcripts after correction for the mass of products (562/235 bp). M, size standard (100-bp ladder). *B*: results for IS1, IS2, and IS4. The ratio of intensity of each band to total is shown on *right*.

and an equal number of both variants were expressed for IS2. In contrast, the deletion variant was primarily expressed for IS4; the ratio for the insertion variant was only 3%.

DISCUSSION

In the present study, we cloned and sequenced the full-length cDNA encoding RyR from unfertilized eggs of *H. pulcherrimus*. The corresponding transcripts of several insertion/deletion variants were detected in the mRNA from these eggs. The deduced amino acid sequence of suRyR showed a reasonable degree of identity with known RyRs along the whole molecule and shares several common structural features. The sea urchin egg homogenates demonstrated cADPR-induced Ca^{2+} release and caffeine-induced Ca^{2+} release, both of which were considered to be mediated through RyR. These results suggest that suRyR may form a functional Ca^{2+} release channel, which might also be involved in cADPR-induced Ca^{2+} release.

The immunologic approaches using anti-RyR antibody have detected a ~380-kDa protein (28) or a ~400-kDa protein (25) as a putative RyR molecule in sea urchin egg microsomes. These proteins showed considerably greater mobility on SDS-polyacrylamide gel electrophoresis than rabbit RyR1. This seems inconsistent with our results that the predicted size of suRyR is 580–600 kDa, which is clearly larger than vertebrate RyRs. It is unlikely that some smaller transcripts are also generated in the eggs, because only a large (>18 kbp) transcript was detected by Northern blot (Fig. 7). Possible explanations for the discrepancy might be as follows: some posttranslational modifications, protein degradation, and difference between species, *Lytechinus* (25, 28) and *Hemicentrotus* (this study).

The COOH-terminal region of RyR is thought to constitute an ion channel with all the essential parts, i.e., pore, gate, and ion-selective filter, since a functional Ca^{2+} release channel can be formed by ~1,000 COOH-terminal amino acids (1). Hydropathy profiles revealed four highly hydrophobic segments, which correspond to the putative transmembrane domains (M1–M4) (47) (Fig. 3*A*). The COOH-terminal region of suRyR showed the highest identity (~60%) with the counterparts of the other RyRs, e.g., rabbit RyR2 and *D. melanogaster* RyR (Fig. 3*C*). Recent studies using mutagenesis identified several functionally important residues on the COOH-terminal sequences (2, 12, 55). These residues were well conserved in suRyR (Fig. 4), suggesting that suRyR may constitute a functional Ca^{2+} release channel that is similar in basic behavior to those of known RyRs. This is consistent with the findings that single ryanodine- or ruthenium red-sensitive cation channel currents, which show gating and conducting properties similar to known RyRs, were recorded from sea urchin egg microsomes (25, 35).

We found several amino acid substitutions in the suRyR sequence that may show polymorphism of the gene (Table 1). In addition, four potential insertion/deletion sites (IS1–IS4) were detected (Table 2). RT-PCR analysis demonstrates the presence of transcripts for these variants in sea urchin eggs (Fig. 8). Thus suRyR has several variants that might show different properties in Ca^{2+} release channel function and its regulation. Among these variant sites, IS3 is notable for its large size (109 residues) and sequence characteristic of a serine cluster (Fig. 5). This stretch is entirely unique, because no homologous sequences were detected in the database by BLAST search. The ratio of IS3-positive variants was estimated to be only 6% of total transcripts in sea urchin eggs (Fig. 8). Because IS3 is located near the COOH-terminal region, it is likely that this sequence may affect channel function. Motif analysis found several potential phosphorylation sites around the serine cluster (Fig. 5). It is possible that conformation of IS3 might change by protein phosphorylation through some signal transduction cascades. Using a heterologous expression system, we are starting a functional study of these insertion/deletion variants of suRyR.

RyR is well known to release Ca^{2+} from sarcoplasmic reticulum to induce muscle contraction in various vertebrate and invertebrate muscles (10, 31, 44). It is reported that the radial muscle of *Asthenosoma* sea urchins was contracted by caffeine (50). We also found caffeine-induced contracture of the lantern muscle from *H. pulcherrimus* sea urchins (data not shown). Thus it is likely that muscle cells of sea urchins may have functional RyR channels. Phylogenetic analysis indicates only one isoform of RyR in sea urchins, as is true of the other invertebrates (Fig. 6). The suRyR we show here may be expressed as functional Ca^{2+} release channels in *H. pulcherrimus* sea urchin muscle cells. It will be interesting to learn whether compositions of the insertion variants differ between eggs and muscles.

Although the cADPR-induced Ca^{2+} release in sea urchin eggs shares many functional properties with CICR through RyRs, there are also several differences between them (22); one of the most striking is the action of CaM. CaM is an essential factor for activation of cADPR-induced Ca^{2+} release in sea urchin eggs: it sensitizes egg microsomes to Ca^{2+} and acts synergistically with cADPR (24, 48). In contrast, the modulatory effects of CaM on the vertebrate RyR channels depend on Ca^{2+} concentrations: activating at a low [Ca^{2+}] and inhibiting at a high [Ca^{2+}] (16, 49). Furthermore, desensitization is a unique property of cADPR-induced Ca^{2+} release in which Ca^{2+} release in sequence application of the reagent is markedly reduced, even if Ca^{2+} stores possess an appreciable amount of Ca^{2+} (5) (Fig. 1*A*). Therefore, one would expect that there are some unique structural features in suRyR that are linked to such functional characteristics. Analysis of the sequence, however, uncovered no particular regions with marked uniqueness in suRyR, except the IS3 insertion and the two divergent regions (D1 and D2). Further studies with chimeric channels of suRyR and other RyRs will address this interesting question.

In mammalian cells, cADPR-induced Ca^{2+} release is thought to be mediated by limited isoforms of RyR, RyR2, and RyR3 (11, 14, 32, 42). This raises the pos-

sibility that suRyR or its partial stretch may be more similar to RyR2 or RyR3 than to RyR1. Amino acid sequence identities of suRyR with the three mammalian RyR isoforms, however, were of similar magnitude (43–45%; Table 3). Phylogenetic analysis clearly demonstrated that suRyR branched from the ancestral RyR of vertebrates before branching the three isoforms of vertebrate RyR (Fig. 6). Thus we have no evidence that suRyR is more similar to RyR2 or RyR3 than to RyR1. Some fundamental differences in the mechanisms of cADPR-induced Ca^{2+} release between mammals and sea urchin eggs have been pointed out (22). In rat pancreatic β-cells, CaM is reported to act through CaM-dependent protein kinase II (45), whereas CaM-kinase II is not essential for CaM action in sea urchin eggs (24). In addition, 100- and 140-kDa proteins, which bind 8-azido-cADPR, were identified as the "cADPR receptor" in the eggs (51), whereas 12.6-kDa FK506-binding protein is proposed to bind cADPR in the β-cells (30). The proteins in the eggs have not been fully characterized and could also be proteolytic fragments of suRyR. Therefore, further studies are required to address whether the cADPR receptor is a separate protein. Nevertheless, the molecular target for cADPR of the eggs seems different from that of the β-cells. Identification of the RyR molecule from sea urchin eggs provides a useful tool with which to explore the detailed mechanisms of cADPR-induced Ca^{2+} release in eggs and mammalian cells.

We thank Dr. S. Kikuchi and staff members at the Marine Biosystems Research Center, Chiba University, for help in collecting sea urchins and preparing eggs. We are grateful to Dr. E. Suzuki (Juntendo University) for help and valuable advice in the cDNA cloning experiments.

This work was supported in part by the Scientific Research Promotion Fund from Promotion and Mutual Aid for Private Schools of Japan Grant 131025 and by the High Technology Research Center Grant from the Ministry of Education, Science, Sports, Culture, and Technology, Japan.

The nucleotide sequence data reported here will appear in the DDBJ, EMBL, and GenBank nucleotide sequence databases with accession number AB051576.

REFERENCES

1. **Bhat MB, Zhao J, Takeshima H, and Ma J.** Functional calcium release channel formed by the carboxyl-terminal portion of ryanodine receptor. *Biophys J* 73: 1329–1336, 1997.
2. **Chen SRW, Ebisawa K, Li X, and Zhang L.** Molecular identification of the ryanodine receptor Ca^{2+} sensor. *J Biol Chem* 273: 14675–14678, 1998.
3. **Chirgwin JM, Przybyla AE, MacDonald RJ, and Rutter WJ.** Isolation of biologically active ribonucleic acid from sources enriched in ribonuclease. *Biochemistry* 18: 5294–5299, 1979.
4. **Clapper DL and Lee HC.** Inositol trisphosphate induces calcium release from nonmitochondrial stores in sea urchin egg homogenates. *J Biol Chem* 260: 13947–13954, 1985.
5. **Clapper DL, Walseth TF, Dargie PJ, and Lee HC.** Pyridine nucleotide metabolites stimulate calcium release from sea urchin egg microsomes desensitized to inositol trisphosphate. *J Biol Chem* 262: 9561–9568, 1987.
6. **Du GG and MacLennan DH.** Functional consequences of mutations of conserved, polar amino acids in transmembrane sequences of the Ca^{2+} release channel (ryanodine receptor) of rabbit skeletal muscle sarcoplasmic reticulum. *J Biol Chem* 273: 31867–31872, 1998.
7. **Endo M.** Calcium release from sarcoplasmic reticulum. *Curr Top Membr Transp* 25: 181–230, 1985.
8. **Felsenstein J.** Evolutionary trees from DNA sequences: a maximum likelihood approach. *Evolution* 39: 783–791, 1981.
9. **Franck JP, Morrissette J, Keen JE, Londraville RL, Beamsley M, and Block BA.** Cloning and characterization of fiber type-specific ryanodine receptor isoforms in skeletal muscles of fish. *Am J Physiol Cell Physiol* 275: C401–C415, 1998.
10. **Franzini-Armstrong C and Protasi F.** Ryanodine receptors of striated muscles: a complex channel capable of multiple interactions. *Physiol Rev* 77: 699–729, 1997.
11. **Galione A, Cui Y, Empson R, Iino S, Wilson H, and Terrar D.** Cyclic ADP-ribose and the regulation of calcium-induced calcium release in eggs and cardiac myocytes. *Cell Biochem Biophys* 28: 19–30, 1998.
12. **Gao L, Balshaw D, Xu L, Tripathy A, Xin C, and Meissner G.** Evidence for a role of the luminal M3-M4 loop in skeletal muscle Ca^{2+} release channel (ryanodine receptor) activity and conductance. *Biophys J* 79: 828–840, 2000.
13. **Graeff RM, Podein RJ, Aarhus R, and Lee HC.** Magnesium ions but not ATP inhibit cyclic ADP-ribose-induced calcium release. *Biochem Biophys Res Commun* 206: 786–791, 1995.
14. **Guse AH, da Silva CP, Berg I, Skapenko AL, Weber K, Heyer P, Hohenegger M, Ashamu GA, Schulze-Koops H, Potter BV, and Mayr GW.** Regulation of calcium signaling in T lymphocytes by the second messenger cyclic ADP-ribose. *Nature* 398: 70–73, 1999.
15. **Hakamata Y, Nakai J, Takeshima H, and Imoto K.** Primary structure and distribution of a novel ryanodine receptor/calcium release channel from rabbit brain. *FEBS Lett* 312: 229–235, 1992.
16. **Ikemoto T, Iino M, and Endo M.** Enhancing effect of calmodulin on Ca^{2+}-induced Ca^{2+} release in the sarcoplasmic reticulum of rabbit skeletal muscle fibres. *J Physiol (Lond)* 487: 573–582, 1995.
17. **Jacobson MK, Coyle DL, Vu CQ, Kim H, and Jacobson EL.** Preparation of cyclic ADP-ribose, 2′-phospho-cyclic ADP-ribose, and nicotinate adenine dinucleotide phosphate: possible second messengers of calcium signaling. *Methods Enzymol* 280: 265–275, 1997.
18. **Kemp BE and Pearson RB.** Protein kinase recognition sequence motifs. *Trends Biochem Sci* 15: 342–346, 1990.
19. **Kozak M.** Compilation and analysis of sequences upstream from the translational start site in eukaryotic mRNAs. *Nucleic Acids Res* 12: 857–872, 1984.
20. **Kretsinger RH.** Calcium coordination and the calmodulin fold: divergent versus convergent evolution. *Cold Spring Harb Symp Quant Biol* 52: 499–510, 1987.
21. **Kyte J and Doolittle RF.** A simple method for displaying the hydropathic character of a protein. *J Mol Biol* 157: 105–132, 1982.
22. **Lee HC.** Mechanisms of calcium signaling by cyclic ADP-ribose and NAADP. *Physiol Rev* 77: 1133–1164, 1997.
23. **Lee HC.** Potentiation of calcium- and caffeine-induced calcium release by cyclic ADP-ribose. *J Biol Chem* 268: 293–299, 1993.
24. **Lee HC, Aarhus R, Graeff R, Gurnack ME, and Walseth TF.** Cyclic ADP ribose activation of the ryanodine receptor is mediated by calmodulin. *Nature* 370: 307–309, 1994.
25. **Lokuta AJ, Darszon A, Beltran C, and Valdivia HH.** Detection and functional characterization of ryanodine receptors from sea urchin eggs. *J Physiol (Lond)* 510: 155–164, 1998.
26. **Martin J, Geromanos S, Tempst P, and Hartl FU.** Identification of nucleotide-binding regions in the chaperonin proteins GroEL and GroES. *Nature* 366: 279–282, 1993.
27. **Marx SO, Reiken S, Hisamitsu Y, Gaburjakova M, Gaburjakove J, Yang YM, Rosemblit N, and Marks AR.** Phosphorylation-dependent regulation of ryanodine receptors: a novel role for leucine and isoleucine zippers. *J Cell Biol* 153: 699–708, 2001.
28. **McPherson SM, McPherson PS, Mathews L, Campbell KP, and Longo FJ.** Cortical localization of a calcium release channel in sea urchin eggs. *J Cell Biol* 116: 1111–1121, 1992.
29. **Nakai J, Imagawa T, Hakamata Y, Shigekawa M, Takeshima H, and Numa S.** Primary structure and functional

expression from cDNA of the cardiac ryanodine receptor/calcium release channel. *FEBS Lett* 271: 169–177, 1990.
30. **Noguchi N, Takasawa S, Nata K, Tohgo A, Kato I, Ikehata F, Yonekura H, and Okamoto H.** Cyclic ADP-ribose binds to FK506-binding protein 12.6 to release Ca^{2+} from islet microsomes. *J Biol Chem* 272: 3133–3136, 1997.
31. **Ogawa Y.** Role of ryanodine receptors. *Crit Rev Biochem Mol Biol* 29: 229–274, 1994.
32. **Okamoto H.** The CD38-cyclic ADP-ribose signaling system in insulin secretion. *Mol Cell Biochem* 193: 115–118, 1999.
33. **Ottini L, Marziali G, Conti A, Charlesworth A, and Sorrentino V.** α and β isoforms of ryanodine receptor from chicken skeletal muscle are the homologues of mammalian RyR1 and RyR3. *Biochem J* 315: 207–216, 1996.
34. **Oyamada H, Murayama T, Takagi T, Iino M, Iwabe N, Miyata T, Ogawa Y, and Endo M.** Primary structure and distribution of ryanodine-binding protein isoforms of the bullfrog skeletal muscle. *J Biol Chem* 269: 17206–17214, 1994.
35. **Perez CF, Marengo JJ, Bull R, and Hidalgo C.** Cyclic ADP-ribose activates caffeine-sensitive calcium channels from sea urchin egg microsomes. *Am J Physiol Cell Physiol* 274: C430–C439, 1998.
36. **Proudfoot NJ and Brownlee GG.** 3′-Noncoding region sequences in eukaryotic messenger RNA. *Nature* 263: 211–214, 1976.
37. **Rhoads AR and Friedberg F.** Sequence motifs for calmodulin recognition. *FASEB J* 11: 331–340, 1997.
38. **Rodney GG, Moore CP, Williams BY, Zhang JZ, Krol J, Pedersen SE, and Hamilton SL.** Calcium binding to calmodulin leads to an N-terminal shift in its binding site on the ryanodine receptor. *J Biol Chem* 276: 2069–2074, 2001.
39. **Saitou N and Nei M.** The neighbor-joining method: a new method for reconstructing phylogenetic trees. *Mol Biol Evol* 4: 406–425, 1987.
40. **Sakube Y, Ando H, and Kagawa H.** An abnormal ketamine response in mutants defective in the ryanodine receptor gene *ryr-1* (*unc-68*) of *Caenorhabditis elegans*. *J Mol Biol* 267: 849–864, 1997.
41. **Saraste M, Sibbald PR, and Wittinghofer A.** The P-loop—a common motif in ATP- and GTP-binding proteins. *Trends Biochem Sci* 15: 430–434, 1990.
42. **Sonnleitner A, Conti A, Bertocchini F, Schindler H, and Sorrentino V.** Functional properties of the ryanodine receptor type 3 (RyR3) Ca^{2+} release channel. *EMBO J* 17: 2790–2798, 1998.
43. **Sorrentino V and Volpe P.** Ryanodine receptors: how many, where and why? *Trends Pharmacol Sci* 14: 98–103, 1993.
44. **Sutko JL and Airey JA.** Ryanodine receptor Ca^{2+} release channels: does diversity in form equal diversity in function? *Physiol Rev* 76: 1027–1071, 1996.
45. **Takasawa S, Ishida A, Nata K, Nakagawa K, Noguchi N, Tohgo A, Kato I, Yonekura H, Fujisawa H, and Okamoto H.** Requirement of calmodulin-dependent protein kinase II in cyclic ADP-ribose-mediated intracellular Ca^{2+} mobilization. *J Biol Chem* 270: 30257–30259, 1995.
46. **Takeshima H, Nishi M, Iwabe N, Miyata T, Hosoya T, Masai I, and Hotta Y.** Isolation and characterization of a gene for a ryanodine receptor/calcium release channel in *Drosophila melanogaster*. *FEBS Lett* 337: 81–87, 1994.
47. **Takeshima H, Nishimura S, Matsumoto T, Ishida H, Kangawa K, Minamino N, Matsuo H, Ueda M, Hanaoka M, Hirose T, and Numa S.** Primary structure and expression from complementary DNA of skeletal muscle ryanodine receptor. *Nature* 339: 439–445, 1989.
48. **Tanaka Y and Tashjian AH Jr.** Calmodulin is a selective mediator of Ca^{2+}-induced Ca^{2+} release via the ryanodine receptor-like Ca^{2+} channel triggered by cyclic ADP-ribose. *Proc Natl Acad Sci USA* 92: 3244–3248, 1995.
49. **Tripathy A, Xu L, Mann G, and Meissner G.** Calmodulin activation and inhibition of skeletal muscle Ca^{2+} release channel (ryanodine receptor). *Biophys J* 69: 106–119, 1995.
50. **Tsuchiya T and Amemiya S.** Studies on the radial muscle of an echinothuriid sea-urchin, *Asthenosoma*. I. Mechanical responses to electrical stimulation and drugs. *Comp Biochem Physiol C Pharmacol Toxicol Endocrinol* 57: 69–73, 1977.
51. **Walseth TF, Aarhus R, Kerr JA, and Lee HC.** Identification of cyclic ADP-ribose-binding proteins by photoaffinity labeling. *J Biol Chem* 268: 26686–26691, 1993.
52. **Whitaker MJ and Steinhardt RA.** Ionic regulation of egg activation. *Q Rev Biophys* 15: 593–666, 1982.
53. **Xiong H, Feng X, Gao L, Xu L, Pasek DA, Seok JH, and Meissner G.** Identification of a two EF-hand Ca^{2+} binding domain in lobster skeletal muscle ryanodine receptor/Ca^{2+} release channel. *Biochemistry* 37: 4804–4814, 1998.
54. **Yamaguchi N, Xin C, and Meissner G.** Identification of apocalmodulin and Ca^{2+}-calmodulin regulatory domain in skeletal muscle Ca^{2+} release channel, ryanodine receptor. *J Biol Chem* 276: 22579–22585, 2001.
55. **Zhao M, Li P, Li X, Zhang L, Winkfein RJ, and Chen SR.** Molecular identification of the ryanodine receptor pore-forming segment. *J Biol Chem* 274: 25971–25974, 1999.
56. **Zorzato F, Fujii J, Otsu K, Phillips M, Green NM, Lai FA, Meissner G, and MacLennan DH.** Molecular cloning of cDNA encoding human and rabbit forms of the Ca^{2+} release channel (ryanodine receptor) of skeletal muscle sarcoplasmic reticulum. *J Biol Chem* 265: 2244–2256, 1990.